Chapter 1

Learning in the Wavelet Domain

In this chapter we move away from the ScatterNet ideas from the previous chapters and instead look at using the wavelet domain as a new space in which to learn. In particular the ScatterNet, and even the learnable ScatterNet proposed in the previous chapter, are built around taking complex magnitudes of the highpass wavelets. This inherently builds invariance to shifts but at the cost of making things smoother. In many ways this was beneficial, as it allowed us to subsample the output and we saw that the scattering layers worked well just before downsampling stages of a CNN. However, we would now like to explore if it is possible and at all beneficial to learn with wavelets without taking the complex magnitude. This means that the frequency support of our activations will remain in the same space in the Fourier domain.

The inspiration to this chapter is the hope that learning in the frequency/wavelet domain may afford simpler filters than learning in the pixel domain. A classic example of this is the first layer filters in AlexNet shown in Figure 1.1. These could be parameterized with only a few nonzero wavelet coefficients, or alternatively, we could take a decomposition of each input channel and keep individual subbands (or equivalently, attenuate other bands), then take the inverse wavelet transform.

Our experiments show that . . . **FINISH ME**

1.1 Related Work

1.1.1 Wavelets as a Front End

Fujieda et. al. use a DWT in combination with a CNN to do texture classification and image annotation [3], [4]. In particular, they take a multiscale wavelet transform of the input image, combine the actviations at each scale independently with learned weights, and feed these back into the network where the activation resolution size matches the subband resolution. The architecture block diagram is shown in Figure 1.2, taken from the original paper. This

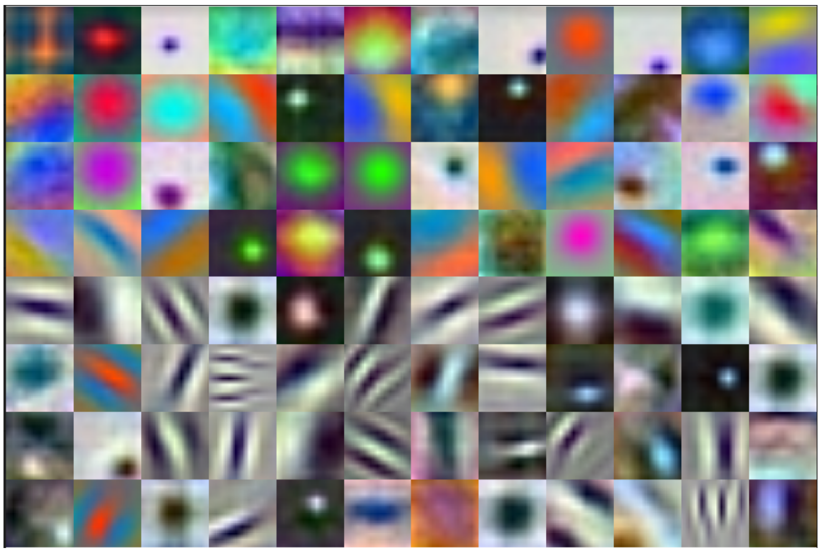

Figure 1.1: **First layer filters of the AlexNet architecture.** The first layer filters of the seminal AlexNet [1] are an inspiration for considering learning filters in the wavelet domain. Each of these 11×11 filters would only require a handful of non zero coefficients in the wavelet domain. The weights shown here were taken from a pretrained network from torchvision [2].

work found that their dubbed 'Wavelet-CNN' could outperform competetive non wavelet based CNNs on both texture classification and image annotation.

Several works also use wavelets in deep neural networks for super-resolution [5] and for adding detail back into dense pixel-wise segmentation tasks [6]. These typically save wavelet coefficients and use them for the reconstruction phase, so are a little less applicable than the first work.

1.1.2 Parameterizing filters in Fourier Domain

In "Spectral Representations for Convolutional Neural Networks" [7], Rippel et. al. explore parameterization of filters in the DFT domain. Note that they do not necessarily do the convolution in the Frequency domain, they simply parameterize a filter $\mathbf{w} \in \mathbb{R}^{F\times C\times K\times K}$ as a set of fourier coefficients $\hat{\mathbf{w}} \in \mathbb{C}^{F\times C\times K\times \lceil K/2 \rceil}$ (the reduced spatial size is a result of enforcing that the inverse DFT of their filter to be real, so the parameterization is symmetric). On the forward pass of the neural network, they take the inverse DFT of $\hat{\mathbf{w}}$ to obtain $\mathbf{w}$ and then convolve this with the input $\mathbf{x}$ as a normal CNN would do.[1].

[1]The convolution may be done by taking both the image and filter back into the fourier space but this is typically decided by the framework, which selects the optimal convolution strategy for the filter and input size. Note that there is not necessarily a saving to be gained by enforcing it to do convolution by product of FFTs, as the FFT size needed for the filter will likely be larger than $K \times K$, which would require resampling the coefficients

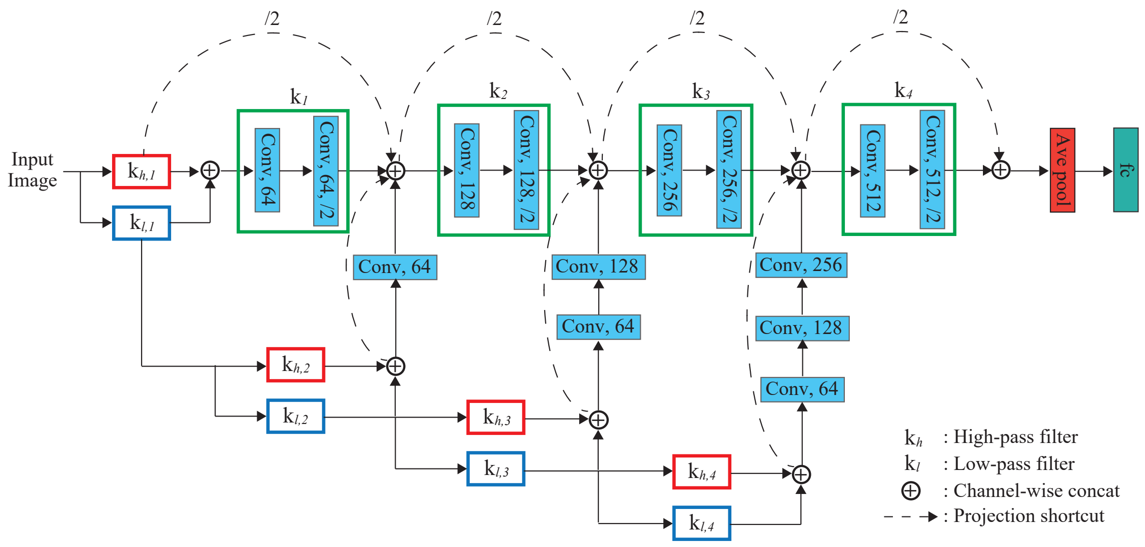

Figure 1.2: **Architecture using the DWT as a frontend to a CNN.** Figure 1 from [4]. Fujieda et. al. take a multiscale wavelet decomposition of the input before passing the input through a standard CNN. They learn convolutional layers independently on each subband and feed these back into the network at different depths, where the resolution of the subband and the network activations match.

1.2 Introduction

We would like to explore the possibility of using the wavelet domain as a space to learn. Unlike the work of [7] which only parameterized filters in the wavelet domain and transformed the filters back to the pixel domain to do convolution, this chapter explores learning wholly in the wavelet domain. I.e., we want to take a wavelet decomposition of the input and learn gains to apply to these coefficients, and optionally return to the pixel domain.

As neural network training involves presenting thousands of training samples on memory limited GPUs, we want our layer to be fast and as memory efficient as possible. To achieve this we would ideally choose to use a critically sampled filter bank implementation. The fast 2-D Discrete Wavelet Transform (DWT) is a possible option, but it has two drawbacks: it has poor directional selectivity and any alteration of wavelet coefficients will cause the aliasing cancelling properties of the reconstructed signal to disappear. Another option is to use the DTℂWT [8]. This comes with a memory overhead which we discuss more in subsubsection 1.5.3.1, but it enables us to have have better directional selectivity and allows for the possibility of returning to the pixel domain with minimal aliasing [9].

We will look at the merits and drawbacks of both options, discuss how to implement them, and finally run some experiments exploring how well these layers work.

1.2.1 Invertible Transforms and Optimization

Note that an important point should be laboured about reparameterizing filters in either the wavelet or Fourier domains. That is that any invertible linear transform of the parameter space will not change the updates if a linear optimization scheme (like standard gradient descent, or SGD with momentum) is used. This is proved in Appendix A.

1.3 Background and Notation

As we now want to consider the DWT and the DTℂWT which are both implemented as filter bank systems, we deviate slightly from the notation in the previous chapter (which was inspired by sampling a continuous wavelet transform).

Firstly, instead of talking about the continuous spatial variable $\mathbf{u}$, we now consider the discrete spatial variable $\mathbf{n} = [n_1, n_2]$. We switch to square brackets to make this clearer. With the new discrete notation, the output of a CNN at layer l is:

$$x^{(l)}[c, \mathbf{n}], \quad c \in \{0, \dots C_l - 1\}, \mathbf{n} \in \mathbb{Z}^2 \tag{1.3.1}$$

where c indexes the channel dimension. We also make use of the 2-D Z-transform to simplify our analysis:

$$X(\mathbf{z}) = \sum_{n_1}\sum_{n_2} x[n_1, n_2] z_1^{-n_1} z_2^{-n_2} = \sum_{\mathbf{n}} x[c, \mathbf{n}] \mathbf{z}^{-\mathbf{n}} \tag{1.3.2}$$

As we are working with three dimensional arrays (two spatial and one channel) but are only doing convolution in two, we introduce a slightly modified 2-D Z-transform which includes the channel index:

$$X(c, \mathbf{z}) = \sum_{n_1}\sum_{n_2} x[c, n_1, n_2] z_1^{-n_1} z_2^{-n_2} = \sum_{\mathbf{n}} x[c, \mathbf{n}] \mathbf{z}^{-\mathbf{n}} \tag{1.3.3}$$

Recall that a typical convolutional layer in a standard CNN gets the next layer's output in a two-step process:

$$y^{(l+1)}[f, \mathbf{n}] = \sum_{c=0}^{C_l - 1} x^{(l)}[c, \mathbf{n}] * h_f^{(l)}[c, \mathbf{n}] \tag{1.3.4}$$

$$x^{(l+1)}[f, \mathbf{u}] = \sigma\left(y^{(l+1)}[f, \mathbf{u}]\right) \tag{1.3.5}$$

In shorthand, we can reduce the action of the convolutional layer in (1.3.4) to $\mathcal{H}$, saying:

$$y^{(l+1)} = \mathcal{H} x^{(l)} \tag{1.3.6}$$

With the new Z-transform notation introduced in (1.3.3), we can rewrite (1.3.4) as:

$$Y^{(l+1)}(f,\mathbf{z}) = \sum_{c=0}^{C_l-1} X^{(l)}(c,\mathbf{z})\, H_f^{(l)}(c,\mathbf{z}) \tag{1.3.7}$$

Note that we cannot rewrite (1.3.5) with Z-transforms as it is a nonlinear operation.

Also recall that with multirate systems, upsampling by M takes $X(z)$ to $X(z^M)$ and downsampling by M takes $X(z)$ to $\frac{1}{M}\sum_{k=0}^{M-1} X(W_M^k z^{1/k})$ where $W_M^k = e^{\frac{j2\pi k}{M}}$. We will drop the M subscript below unless it is unclear of the sample rate change, simply using W^k.

1.3.1 DWT Notation

In 2-D, a J scale DWT gives $3J+1$ coefficients, 3 sets of bandpass coefficients for each scale, representing the horizontal, vertical and diagonal regions of the frequency plane, and 1 set of lowpass coefficients at the final scale. Let us refer to the DWT wavelet coefficients with the typewriter font $\mathtt{u}$ and write the J scale DWT as:

$$\mathrm{DWT}_J(x) = \mathtt{u}_{lp}, \{\mathtt{u}_{j,k}\}_{1\leq j\leq J, 1\leq k\leq 3} \tag{1.3.8}$$

If x is a batch of 2-D images with multiple channels, the DWT is done indpendently on each channel in each minibatch sample. I.e. if the input is a minibatch of N samples with C channels of images of spatial size $H\times W$, then $x\in\mathbb{R}^{N\times C\times H\times W}$ and:

$$\mathtt{u}_{lp} \in \mathbb{R}^{N\times C\times \frac{H}{2^J}\times\frac{W}{2^J}} \tag{1.3.9}$$

$$\mathtt{u}_{j,k} \in \mathbb{R}^{N\times C\times \frac{H}{2^J}\times\frac{W}{2^J}} \tag{1.3.10}$$

Sometimes we may want to refer to all of the subband coefficients at a single scale with one variable, in which case we will simply drop the k subscript and call them $\mathtt{u}_j$. Additionally if we want to refer to all the coefficients (lowpass and bandpass) we will call them $\mathtt{u}$.

1.3.2 DT$\mathbb{C}$WT Notation

Unlike the DWT, a J scale DT$\mathbb{C}$WT gives $6J+1$ coefficients, 6 sets of complex bandpass coefficients for each scale (representing the oriented bands from 15 to 165 degrees) and 1 set of real lowpass coefficients.

Although we will only ever use either the DWT or the DT$\mathbb{C}$WT, to avoid confusion we use a regular font u to refer to the DT$\mathbb{C}$WT coefficients of x:

$$\mathrm{DT\mathbb{C}WT}_J(x) = u_{lp}, \{u_{j,k}\}_{1\leq j\leq J, 1\leq k\leq 6} \tag{1.3.11}$$

Each of these coefficients then has size:

$$u_{lp} \in \mathbb{R}^{N\times C\times \frac{H}{2^{J-1}} \times \frac{W}{2^{J-1}}} \tag{1.3.12}$$

$$u_{j,k} \in \mathbb{C}^{N\times C\times \frac{H}{2^{J}} \times \frac{W}{2^{J}}} \tag{1.3.13}$$

Note that the lowpass coefficients are twice as large as in a fully decimated transform, a feature of the redundancy of the DT$\mathbb{C}$WT.

Again if we ever want to refer to all the subbands at a given scale, we will drop the k subscript and call them u_j. Likewise, u refers to the whole set of DT$\mathbb{C}$WT coefficients.

When we want to be agnostic of the chosen transform type, we use $\mathcal{W}$ and $\mathcal{W}^{-1}$ to denote the forward and inverse transform.

1.4 Parameterizing Filters in the Wavelet Domain

This is a simple extension of the work done by Rippel et. al. who parameterize their filters in the Fourier domain. As with the Fourier parameterization, a Wavelet parameterization introduces some challenges. Most notably that any filters parameterized with a decimated wavelet transform will naturally want to have a spatial support of a power of 2 whereas most convolutional filters in CNNs have an odd spatial support, typically of size 3 (and maybe more for earlier layers). This is done for a very good reason too, in that we do not want our filters to shift the activations.

How much does Rippel talk about reparameterizing in the fourier domain?

1.4.1 DT$\mathbb{C}$WT parameterization

1.4.2 DWT parameterization

1.5 The Wavelet Gain Layer

At the beginning of each stage of a neural network we have the activations $x^{(l)}$. Naturally, all of these activations have their equivalent DWT coefficients $\mathtt{u}^{(l)}$ and DT$\mathbb{C}$WT coefficients $u^{(l)}$.

From (1.3.4), convolutional layers also have intermediate activations $y^{(l)}$. Let us differentiate these from the x coefficients and modify (1.3.8) and (1.3.11) to say the DWT of $y^{(l)}$ gives $\mathtt{v}$ and the DT$\mathbb{C}$WT of $y^{(l)}$ gives v.

We now propose the wavelet gain layers $\mathtt{G}$ and G for the DWT and DT$\mathbb{C}$WT respectively, or $\mathcal{G}$ for an implementation agnostic layer. The name 'gain layer' comes from the inspiration for this chapter's work, in that the first layer of CNN could be nearly done in the wavelet domain by setting subband gains to 0 and 1.

The gain layer $\mathcal{G}$ can be used instead of a convolutional layer. It is designed to work on the wavelet coefficients of an activation, $\mathtt{u}$ and u to give outputs $\mathtt{v}$ and v.

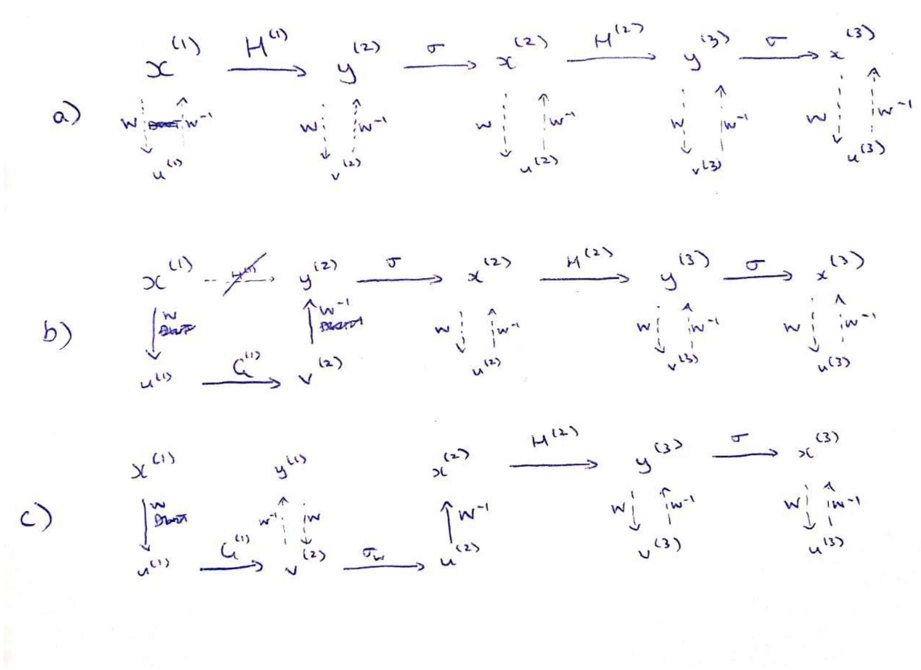

Figure 1.3: **Proposed new forward pass in the wavelet domain.** Two network layers with some possible options for processing. Solid lines denote the evaluation path and dashed lines indicate relationships. In (a) we see a regular convolutional neural network. We have included the dashed lines to make clear what we are denoting as u and v with respect to their equivalents x and y. In (b) we get to $y^{(2)}$ through a different path. First we take the wavelet transform of $x^{(1)}$ to give $u^{(1)}$, apply a wavelet gain layer $\mathcal{G}^{(1)}$, and take the inverse wavelet transform to give $y^{(2)}$. The cross through $\mathcal{H}^{(1)}$ indicates that this path is no longer present. Note that there may not be any possible $\mathcal{G}^{(1)}$ to make $y^{(2)}$ from (b) equal $y^{(2)}$ from (a). In (c) we have stayed in the wavelet domain longer, and applied a wavelet nonlinearity σ_w to give $u^{(2)}$. We then return to the pixel domain to give $x^{(2)}$ and continue on from there in the pixel domain.

This can be seen as breaking the convolutional path in Figure 1.3 and taking a new route to get to the next layer's coefficients. From here, we can return to the pixel domain by taking the corresponding inverse wavelet transform $\mathcal{W}^{-1}$. Alternatively, we can stay in the wavelet domain and apply a wavelet based nonlinearity σ_w to give the next layer's u coefficients. Ultimately we would like to explore architecture design with arbitrary sections in the wavelet and pixel domain, but to do this we must first explore:

- How effective $\mathcal{G}$ is at replacing $\mathcal{H}$.

- How effective σ_w is at replcaing σ.

1.5.1 The DWT Gain Layer

As mentioned previously, modifying the wavelet coefficients of a critically sampled DWT will necessarily result in a loss of the aliasing cancelling properties. However, in a deep neural network, this is not as obviously a bad thing as it is for denoising or deconvolution. For this reason, we note that there may be a problem in using a DWT, but proceed nonetheless.

For each subband in our J scale system, we introduce a gain term $\mathtt{g}$. Let us specify our input $\mathtt{u}$ has C_l channels, and we would like our output $\mathtt{v}$ to have C_{l+1} channels, then $\mathtt{g}$ is made up of:

$$\mathtt{g}_{lp} \in \mathbb{R}^{C_{l+1}\times C_l \times k_{lp} \times k_{lp}} \tag{1.5.1}$$

$$\mathtt{g}_{1,1} \in \mathbb{R}^{C_{l+1}\times C_l \times k_1 \times k_1} \tag{1.5.2}$$

$$\mathtt{g}_{1,2} \in \mathbb{R}^{C_{l+1}\times C_l \times k_1 \times k_1} \tag{1.5.3}$$

$$\vdots$$

$$\mathtt{g}_{J,3} \in \mathbb{R}^{C_{l+1}\times C_l \times k_J \times k_J} \tag{1.5.4}$$

Note that we have allowed for different kernel spatial sizes for the lowpass and for each bandpass scale $\mathtt{g}_j$. This is to allow for the flexibility of putting more emphasis on certain frequency areas if desired.

With these gains, we define $\mathtt{v} = \mathtt{Gu}$ to be:

$$\mathtt{v}_{lp}[f,\mathbf{n}] = \sum_{c=0}^{C_l-1} \mathtt{u}_{lp}[c,\mathbf{n}] * \mathtt{g}_{lp}[f,c,\mathbf{n}] \tag{1.5.5}$$

$$\mathtt{v}_{1,1}[f,\mathbf{n}] = \sum_{c=0}^{C_l-1} \mathtt{u}_{1,1}[c,\mathbf{n}] * \mathtt{g}_{1,1}[f,c,\mathbf{n}] \tag{1.5.6}$$

$$\mathtt{v}_{1,2}[f,\mathbf{n}] = \sum_{c=0}^{C_l-1} \mathtt{u}_{1,2}[c,\mathbf{n}] * \mathtt{g}_{1,2}[f,c,\mathbf{n}] \tag{1.5.7}$$

$$\vdots$$

$$\mathtt{v}_{J,3}[f,\mathbf{n}] = \sum_{c=0}^{C_l-1} \mathtt{u}_{J,3}[c,\mathbf{n}] * \mathtt{g}_{J,3}[f,c,\mathbf{n}] \tag{1.5.8}$$

I.e., we do independent mixing at each of the different subbands. For 1×1 kernels, this is simply a matrix multiply of the wavelet coefficients. This is shown visually in 1.8a.

1.5.1.1 The Output

To explore the action of the gain layer $\mathtt{G}$ on DWT coefficients, let use examine a 1-D, single scale, and single channel system. We want to find the action of the layer without any

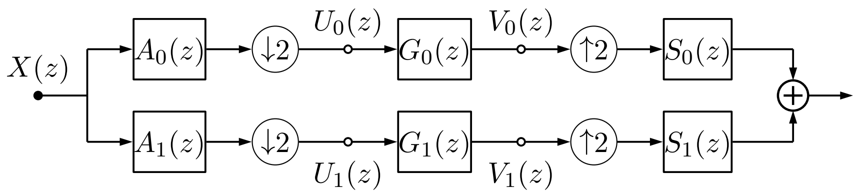

Figure 1.4: **Block Diagram of 1-D DWT Gain Layer.** Here we show the low and highpass for a single scale 1-D DWT, Gain Layer and inverse DWT. The gain layer has gains $\mathtt{g}_0$ and $\mathtt{g}_1$.

nonlinearities, i.e.,

$$y = \mathcal{W}^{-1}\mathtt{G}\mathcal{W}x \tag{1.5.9}$$

or the path taken in Figure 1.3b.

Let us call the low and highpass analysis filters of the DWT A_0 and A_1, and the synthesis filters S_0 and S_1 (these are normally called H and G, but we keep those letters reserved for the CNN and gain layer filters). From the perfect reconstruction property of the DWT, we know

$$A_0(z)S_0(z) + A_1(z)S_1(z) = 2 \tag{1.5.10}$$

and from the aliasing cancellation property of the DWT, we know:

$$A_0(-z)S_0(z) + A_1(-z)S_1(z) = 0 \tag{1.5.11}$$

If we add in gains G_0 and G_1 to the low and highpass coefficients, as shown in Figure 1.4, then the output is:

$$\begin{aligned} Y(z) = &\frac{1}{2}X(z)\left[A_0(z)S_0(z)G_0(z^2) + A_1(z)S_1(z)B(z^2)\right] + \\ &\frac{1}{2}X(-z)\left[A_0(-z)S_0(z)G_0(z^2) + A_1(-z)S_1(z)G_1(z^2)\right] \end{aligned} \tag{1.5.12}$$

If we let $D(z) = G_1(z^2) - G_0(z^2)$ then the above becomes:

$$Y(z) = \frac{1}{2}X(z)\left[A_0(z)S_0(z)G_0(z^2) + A_1(z)S_1(z)G_1(z^2)\right] + \frac{1}{2}X(-z)D(z)A_1(-z)S_1(z) \tag{1.5.13}$$

1.5.1.2 Backpropagation

We start with the commonly known property that for a convolutional block, the gradient with respect to the input is the gradient with respect to the output convolved with the time reverse of the filter. More formally, if $Y(z) = H(z)X(z)$:

$$\Delta X(z) = H(z^{-1})\Delta Y(z) \tag{1.5.14}$$

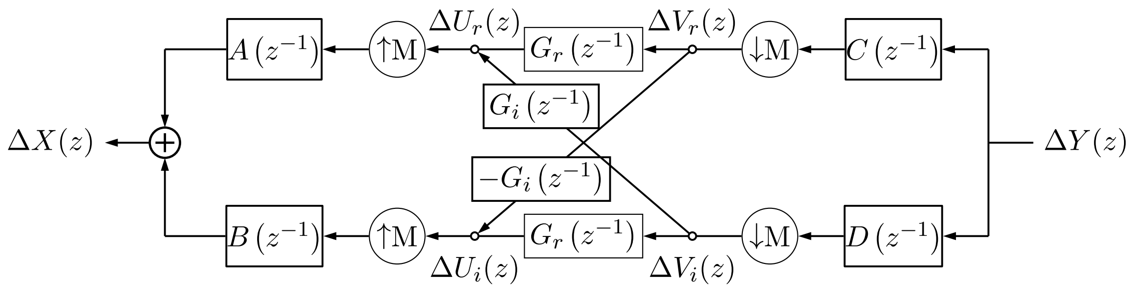

Figure 1.5: **Forward and backward block diagrams for** DTℂWT **gain layer.** Based on Figure 4 in [9]. Ignoring the G gains, the top and bottom paths (through A, C and B, D respectively) make up the the real and imaginary parts for *one subband* of the dual tree system. Combined, $A + jB$ and $C - jD$ make the complex filters necessary to have support on one side of the Fourier domain (see Figure 1.7). Adding in the complex gain $G_r + jG_i$, we can now attenuate/shape the impulse response in each of the subbands. To allow for learning, we need backpropagation. The bottom diagram indicates how to pass gradients $\Delta Y(z)$ through the layer. Note that upsampling has become downsampling, and convolution has become convolution with the time reverse of the filter (represented by z^{-1} terms).

where $H(z^{-1})$ is the Z-transform of the time/space reverse of $H(z)$, $\Delta Y(z) \triangleq \frac{\partial L}{\partial Y}(z)$ is the gradient of the loss with respect to the output, and $\Delta X(z) \triangleq \frac{\partial L}{\partial X}(z)$ is the gradient of the loss with respect to the input.

Assume we already have access to the quantity $\Delta Y(z)$ (this is the input to the backwards pass). **??** illustrates the backpropagation procedure. An interesting result is that for orthogonal wavelet transforms, $S(z^{-1}) = A(z)$, so the backwards pass of an inverse wavelet transform is equivalent to doing a forward wavelet transform. Similarly, the backwards pass of the forward transform is equivalent to doing the inverse transform. The weight update gradients are then calculated by finding $\Delta V_i(z) = S_i(z^{-1})Y(z)$ for $i = 0,\ 1$, and then convolving with the time reverse of the saved wavelet coefficients from the forward pass - $U_i(z^{-1})$.

$$\Delta G_i(z) = \Delta V_i(z) U_i(z^{-1}) \tag{1.5.15}$$

Unsurprisingly, the passthrough gradients have similar form to (1.5.13)

$$\Delta X(z) = \frac{1}{2}\Delta Y(z)\left[A_0(z)S_0(z)G_0(z^{-2}) + A_1(z)S_1(z)G_1(z^{-2})\right] + \frac{1}{2}\Delta Y(-z)D(z)A_1(-z)S_1(z) \tag{1.5.16}$$

Note that we only need to evaluate (1.5.15), (1.5.16) over the support of $G(z)$ i.e., if it is a single number we only need to calculate $\Delta G(z)|_{z=0}$.

1.5.1.3 The DTℂWT Gain Layer

The DTℂWT gain layer is the same in principle to the action of the DWT gain layer, but due to the different properties of the two transforms, the implementation is slightly different. Now that we have the framework for applying a complex gain at one subband, we can extend this to all of the subbands in the DTℂWT. We also reintroduce the channel dimension.

To do the mixing across the C_l channels at each subband, giving C_{l+1} output channels, we introduce the learnable filters:

$$g_{lp} \in \mathbb{R}^{C_{l+1}\times C_l \times k_{lp}\times k_{lp}} \tag{1.5.17}$$

$$g_{1,1} \in \mathbb{C}^{C_{l+1}\times C_l \times k_1\times k_1} \tag{1.5.18}$$

$$g_{1,2} \in \mathbb{C}^{C_{l+1}\times C_l \times k_1\times k_1} \tag{1.5.19}$$

$$\vdots$$

$$g_{J,6} \in \mathbb{C}^{C_{l+1}\times C_l \times k_J\times k_J} \tag{1.5.20}$$

where k, k are the sizes of the mixing kernels. These could be 1×1 for simple gain control, or could be larger, say 3×3, to do more complex filtering on the subbands.

With these gains we define $v = Gu$ to be:

$$v_{lp}[f,\mathbf{n}] = \sum_{c=0}^{C_l-1} u_{lp}[c,\mathbf{n}] * g_{lp}[f,c,\mathbf{n}] \tag{1.5.21}$$

$$v_{1,1}[f,\mathbf{n}] = \sum_{c=0}^{C_l-1} u_{1,1}[c,\mathbf{n}] * g_{1,1}[f,c,\mathbf{n}] \tag{1.5.22}$$

$$v_{1,2}[f,\mathbf{n}] = \sum_{c=0}^{C_l-1} u_{1,2}[c,\mathbf{n}] * g_{1,2}[f,c,\mathbf{n}] \tag{1.5.23}$$

$$\vdots$$

$$v_{J,6}[f,\mathbf{n}] = \sum_{c=0}^{C_l-1} u_{J,6}[c,\mathbf{n}] * g_{J,6}[f,c,\mathbf{n}] \tag{1.5.24}$$

Note that for complex signals a, b the convolution $a*b$ is defined as $(a_r * b_r - a_i * b_i) + j(a_r * b_i + a_i * b_r)$. This is shown in Figure 1.8b.

1.5.1.4 The Output

Unlike the DWT gain layer, the DTℂWT gain layer can achieve aliasing cancelling and therefore has a transfer function. The proof of this is done in Appendix B.

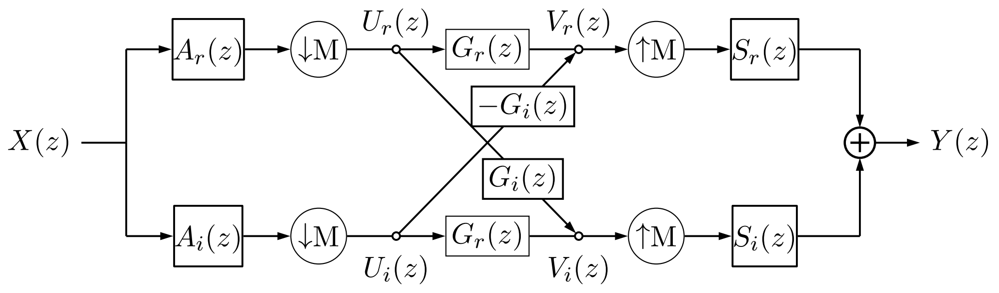

Figure 1.6: **Block Diagram of 1-D** DTℂWT **Gain Layer.** Here we show the real and imaginary trees for a single subband. Note that while it may look similar to Figure 1.4, this diagram represents the two trees for one subband rather than a single tree with a pair of subbands. The gain layer does a complex multiply, using both the real and imaginary parts of the decomposed signal. This preserves the shift invariance of the DTℂWT for the reconstructed signal Y.

For a single subband in the DTℂWT, the gain layer uses a complex learned weight g, but otherwise produces the output v in much the same way as the DWT gain layer. Figure 1.6 shows a single subband DTℂWT based gain layer. The output of this layer is:

$$Y(z) = \frac{2}{M}X(z)\left[G_r(z^M)\left(A_r(z)S_r(z) + A_i(z)S_i(z)\right) + G_i(z^M)\left(A_r(z)S_i(z) - A_i(z)S_r(z)\right)\right] \tag{1.5.25}$$

See Appendix B for the derivation. The G_r term modifies the subband gain $A_rS_r + A_iS_i$ and the G_i term modifies its Hilbert Pair $A_rS_i - A_iS_r$. Figure 1.7 show the contour plots for the frequency support of each of these subbands. The complex gain g can be used to reshape the frequency response for each subband independently.

1.5.1.5 Backpropagation

If H were complex, the first term in Equation 1.5.14 would be $\bar{H}(1/\bar{z})$, but as each individual block in the DTℂWT is purely real, we can use the simpler form $H(z^{-1})$.

Again, let us calculate $\Delta V_r(z)$ and $\Delta V_i(z)$ by backpropagating $\Delta Y(z)$ through the inverse DTℂWT. Again this is the same as doing the forward DTℂWT on $\Delta Y(z)$. Then the weight update equations are:

$$\Delta G_r(z) = \Delta V_r(z)U_r(z^{-1}) + \Delta V_i(z)U_i(z^{-1}) \tag{1.5.26}$$
$$\Delta G_i(z) = -\Delta V_r(z)U_i(z^{-1}) + \Delta V_i(z)U_r(z^{-1}) \tag{1.5.27}$$

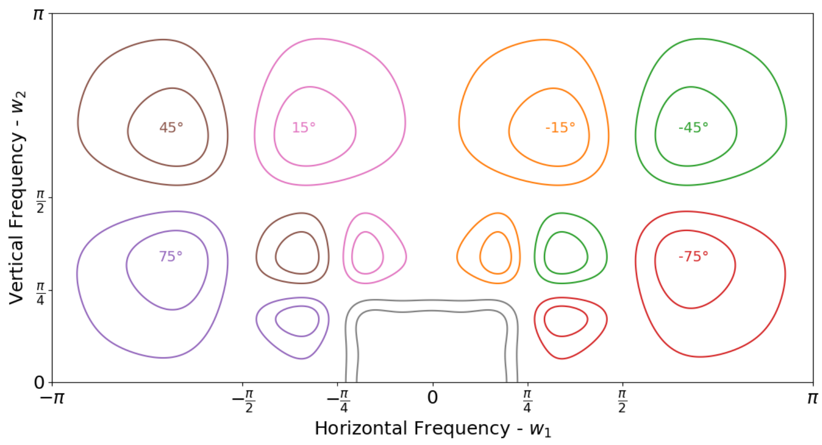

(a)

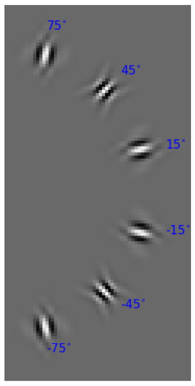

(b)

Figure 1.7: DTℂWT **subbands.** (a) -1dB and -3dB contour plots showing the support in the Fourier domain of the 6 subbands of the DTℂWT at scales 1 and 2, and the scale 2 lowpass. These are the product of the single side band filters $P(z)$ and $Q(z)$ from Theorem B.1. (b) The pixel domain impulse responses for the second scale wavelets. The Hilbert pair for each wavelet is the underlying sinusoid phase shifted by 90 degrees.

The passthrough equations have similar form to (1.5.25):

$$\Delta X(z) = \frac{2\Delta Y(z)}{M}\left[G_r(z^{-M})\left(A_r(z)S_r(z) + A_i(z)S_i(z)\right) + jG_i(z^{-M})\left(A_r(z)S_i(z) - A_i(z)S_r(z)\right)\right] \tag{1.5.28}$$

1.5.2 Examples

Figure 1.9 show example impulse responses of our layer for both the DWT and DTℂWT systems. The DWT outputs come from three random variables: a 1×1 convolutional weight applied to each of the low-high, high-low and high-high subbands. The DTℂWT outputs come from twelve random variables. Again a 1×1 convolutional weight, but now applied to six complex subbands. Our experiments have shown that the distribution of the normalized cross-correlation between 512 of such randomly generated shapes for the DWT matches the distribution for random vectors with roughly 2.8 degrees of freedom (c.f. 3 random variables in the layer). Similarly for the DTℂWT, the distribution of the normalized cross-correlation matches the distribution for random vectors with roughly 11.5 degrees of freedom (c.f. 12 random variables in the layer). This is particularly reassuring for the DTℂWT as it is showing that there is still representatitve power despite the redundancy of the transform.

1.5.3 Implementation Details

Before analyzing its performance, we compare the implementation properties of our two new proposed layers (for the DWT and DTℂWT) to a standard convolutional layer.

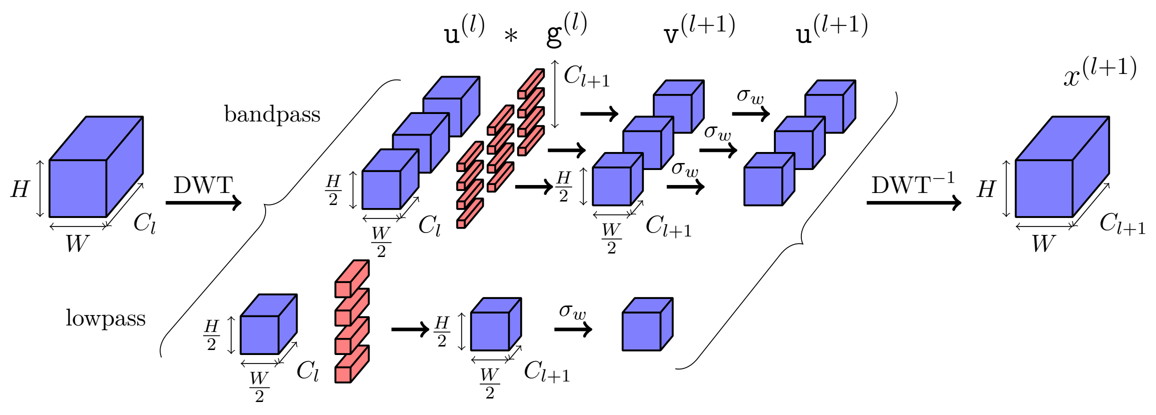

(a)

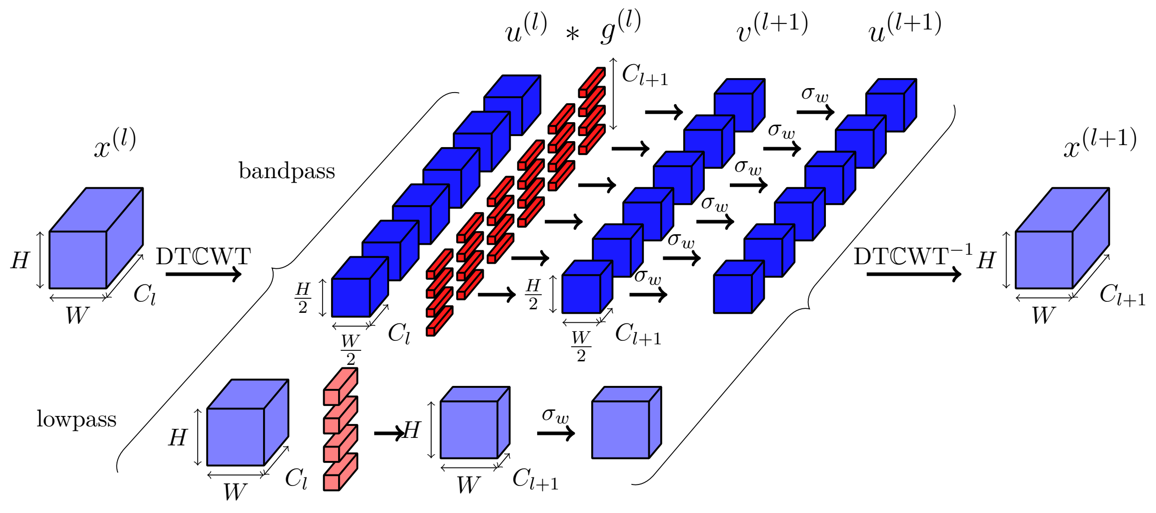

(b)

Figure 1.8: **Block diagrams of proposed method to learn in the wavelet domain.** Activations are shaded blue and learned parameters red. Darker shades of blue and red indicate complex valued activations and weights, whereas the lighter shades indicate purely real values. The input $x^{(l)} \in \mathbb{R}^{C_l \times H \times W}$ is taken into the wavelet domain and each subband is mixed independently with C_{l+1} sets of convolutional filters (this is what we call the 'wavelet gain layer'. After mixing, a possible wavelet nonlinearity σ_w is applied to the subbands, before returning to the pixel domain with an inverse wavelet transform. (a) shows the system in the DWT domain. The DWT has fewer coefficients, and the gain layer requires fewer parameters; this is the simpler layer. (b) shows the DTℂWT based system. With 6 complex subbands and a larger lowpass, this is the more complex layer.

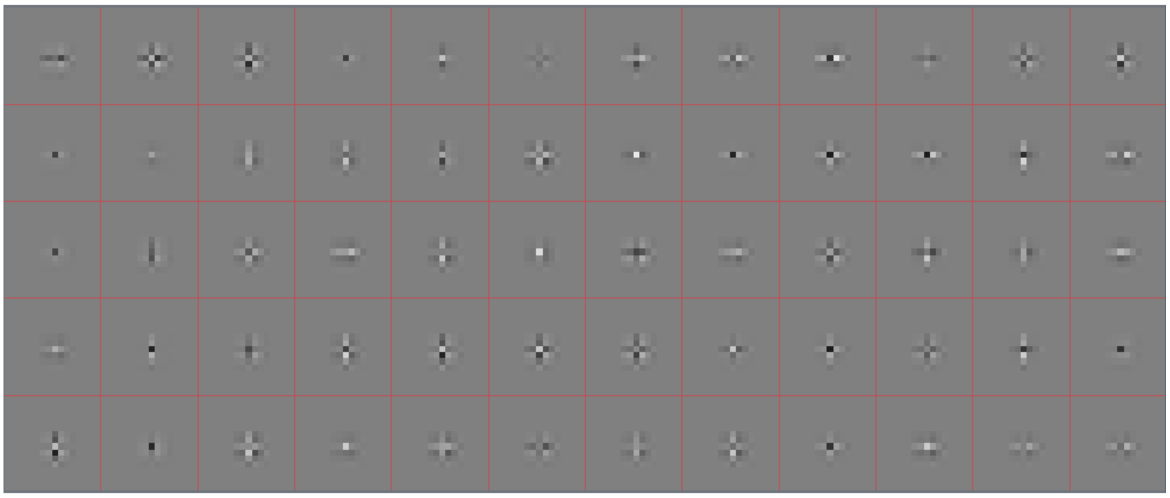

(a)

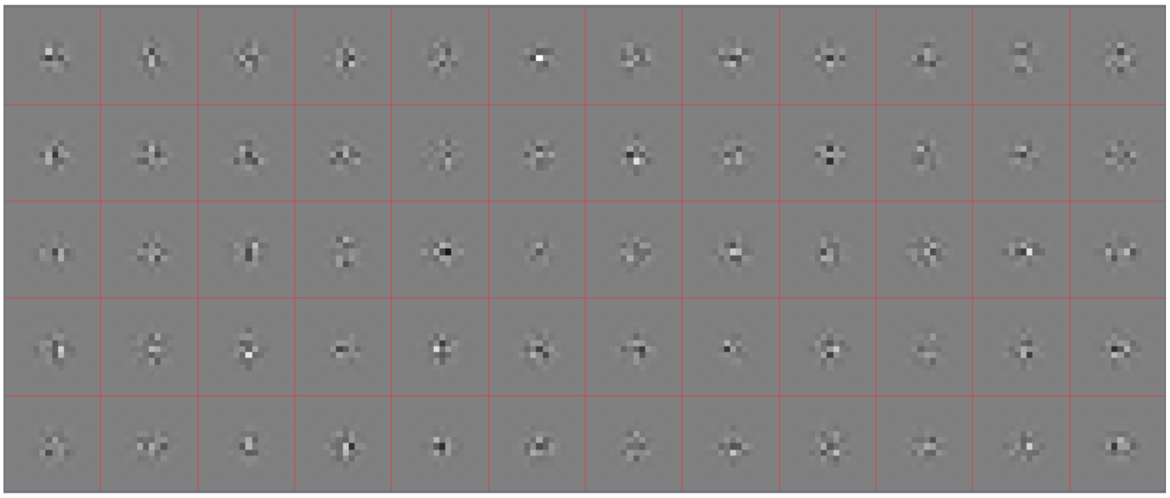

(b)

Figure 1.9: **Example outputs from an impulse input for the proposed gain layers.** Example outputs $y = \mathcal{W}^{-1}\mathcal{G}\mathcal{W}x$ for an impulse x for both the DWT and DT$\mathbb{C}$WT based systems. (a) shows the outputs y when x is an impulse, $\mathcal{W}$ is the DWT with a 'db2' wavelet family and $\mathcal{G} = \mathtt{G}$ is the DWT gain layer. The gain layer weights $\mathtt{g}_{lp}$ coefficients are set to 0 and $\mathtt{g}_1$ coefficients have spatial size 1×1 and are sampled independently from a random normal of variance 1. The 60 samples come from 60 different random initializations. (b) shows the output y for a DT$\mathbb{C}$WT based system. Again, $g_{lp} = 0$ and g_1 has spatial size 1×1. The 12 values in g_1 are independently sampled from a random normal of variance 1.

1.5.3.1 Parameter Memory Cost

A standard convolutional layer with C_l input channels, C_{l+1} output channels and kernel size $L \times L$ has $L^2 C_l C_{l+1}$ parameters, with $L = 3$ or $L = 5$ common choices for the spatial size.

$$\#\text{conv params} = 9 C_l C_{l+1} \tag{1.5.29}$$

We must choose the spatial sizes of both the lowpass and bandpass mixing kernels. In our work, we set:

- The spatial support of the lowpass filters for the DWT gain layer to be 3×3 and the support of the bandpass layers to be 1×1.
- The spatial support of the lowpass filters for the DT$\mathbb{C}$WT gain layer to be 1×1 and the support of the complex bandpass filters to be 1×1.

Further, we limit ourselves initially to only considering a single scale transform. If we wish, we can learn larger spatial sizes to have more complex attenuation/magnification of the subbands. We also can use more than one wavelet scale.

This means that for the DWT layer, the number of parameters is:

$$\#\text{DWT params} = (3 + 3^2) C_l C_{l+1} = 12 C_l C_{l+1} \tag{1.5.30}$$

And for the DT$\mathbb{C}$WT layer, the number of parameters is:

$$\#\text{DT}\mathbb{C}\text{WT params} = (2 \times 6 + 1) C_l C_{l+1} = 13 C_l C_{l+1} \tag{1.5.31}$$

These are both slightly larger than the $9 C_l C_{l+1}$ parameters used in a standard 3×3 convolution, but as Figure 1.9 shows, the spatial support of the full filter is larger than an equivalent one parameterized in the filter domain.

Note that using a second scale ($J = 2$) with 1×1 filters would increase (1.5.30) to $15 C_l C_{l+1}$ and (1.5.31) to $25 C_l C_{l+1}$.

1.5.3.2 Activation Memory Cost

A standard convolutional layer needs to save the activation $x^{(l)}$ to convolve with the backpropagated gradient $\frac{\partial L}{\partial y^{(l+1)}}$ on the backwards pass (to give $\frac{\partial L}{\partial w^{(l)}}$). For an input with C_l channels of spatial size $H \times W$, this means

$$\#\text{conv floats} = H W C_l \tag{1.5.32}$$

Our layers require us to save the wavelet coefficients u_{lp} and $u_{j,k}$ for updating the g terms as in (1.5.15) and (1.5.26), (1.5.27). For the critically sampled DWT, this requires:

$$\#\text{DWT floats} = HWC_l \tag{1.5.33}$$

to be saved for the backwards pass. For the $4:1$ redundant DT$\mathbb{C}$WT, this requires:

$$\#\text{DT}\mathbb{C}\text{WT floats} = 4HWC_l \tag{1.5.34}$$

to be saved for the backwards pass. You can see this difference from the difference in the block diagrams in Figure 1.8.

Note that a single scale DT$\mathbb{C}$WT gain layer requires 16/7 times as many floats to be saved as compared to the invariant layer of the previous chapter. The extra cost of this comes from two things. Firstly, we keep the real and imaginary components for the bandpass (as opposed to only the magnitude), meaning we need $3HWC_l$ floats, rather than $\frac{3}{2}HWC_l$. Additionally, the lowpass was downsampled in the previous chapter, requiring only $\frac{1}{4}HWC_l$, whereas we keep the full sample rate costing HWC_l.

If memory is an issue and the computation of the DT$\mathbb{C}$WT is very fast, then we only need to save the $x^(l)$ coefficients and can calculate the u's on the fly during the backwards pass. Note that a two scale DT$\mathbb{C}$WT gain layer would still only require $4HWC_l$ floats.

1.5.3.3 Computational Cost

A standard convolutional layer with kernel size $L \times L$ needs L^2C_{l+1} multiplies per input pixel (of which there are $C_l \times H \times W$).

For the DWT with Daubechies 2 filters, the forward and inverse transform only require about 6 multiplies per input pixel. The mixing is then done at a reduced spatial resolution. For our proposed kernel sizes of 3×3 for the lowpass and 1×1 for the bandpass, the DWT gain layer requires:

$$\#\text{DWT mults/pixel} = \underbrace{\frac{3}{4}C_{l+1}}_{\text{bandpass}} + \underbrace{\frac{3^2}{4}C_{l+1}}_{\text{lowpass}} + \underbrace{6}_{\text{DWT}} + \underbrace{6}_{\text{DWT}^{-1}} = 4C_{l+1} + 12 \tag{1.5.35}$$

This is smaller than a standard 3×3 convolutional layer using $9C_{l+1}$ multiplies per pixel.

For the DT$\mathbb{C}$WT, the overhead calculations are the same as in **??**, so we will omit their derivation here. The mixing is however different, requiring complex convolution for the bandpass coefficients, and convolution over a higher resolution lowpass. The bandpass has one quarter spatial resolution at the first scale, but this is offset by the $4:1$ cost of complex multiplies compared to real multiplies. Again assuming we have set $J = 1$ and $k_{lp} = 3$ then the total cost for the gain layer is:

$$\#\text{DT}\mathbb{C}\text{WT mults/pixel} = \underbrace{\frac{6\times 4}{4}C_{l+1}}_{\text{bandpass}} + \underbrace{C_{l+1}}_{\text{lowpass}} + \underbrace{36}_{\text{DT}\mathbb{C}\text{WT}} + \underbrace{36}_{\text{DT}\mathbb{C}\text{WT}^{-1}} = 7C_{l+1} + 72 \tag{1.5.36}$$

This is marginally smaller than a 3×3 convolutional layer.

1.5.3.4 Parameter Initialization

For both layer types we use the Glorot Initialization scheme [10] with $a = 1$:

$$g_{ij} \sim U\left[-\sqrt{\frac{6}{(C_l + C_{l+1})k^2}}, \sqrt{\frac{6}{(C_l + C_{l+1})k^2}}\right] \tag{1.5.37}$$

where k is the kernel size.

1.6 Gain Layer Experiments

To explore the effectiveness of our gain layer, we do a similar ablation study to **??** on CIFAR-10, CIFAR-100 and Tiny ImageNet. We use the same reference network so that we can also compare the wavelet gain layer to the invariant layer (see **??**). We also use the same naming technique, calling a network 'gainX' means that the 'convX' layer was replaced with a wavelet gain layer, but otherwise keeping the rest of the architecture the same.

In this section, we are only exploring the wavelet gain layer and not any wavelet nonlinearities. This equates to the path shown in Figure 1.3b. I.eẇe are taking wavelet transforms of inputs, applying the gain layer and taking inverse wavelet transforms to do a ReLU in the pixel space. In cases like 'gainA, gainB' from **??**, we go in and out of the wavelet layer twice.

We train all our networks for with stochastic gradient descent with momentum. The initial learning rate is 0.5, momentum is 0.85, batch size $N = 128$ and weight decay is 10^{-4}. For CIFAR-10/CIFAR-100 we scale the learning rate by a factor of 0.2 after 60, 80 and 100 epochs, training for 120 epochs in total. For Tiny ImageNet, the rate change is at 18, 30 and 40 epochs (training for 45 in total).

Table 1.1 lists the results from these experiments. These show a promising start to this work. We can get an improvement in accuracy by over a percent when we use the gain layer **Finish me when results are done**.

Unlike the scatternet inspired invariant layer from the previous chapter, the gain layer does naturally downsample the output, so we are able to stack more of them? Maybe.

Table 1.1: **Results for testing VGG like architecture with convolutional and wavelet gain layers on several datasets.** An architecture with 'gainX' means the equivalent convolutional layer 'convX' from **??** was swapped for our proposed layer. The top row is the reference architecture using all convolutional layers. The DWT architecture takes a single scale DWT of the activations at the given layer, and mixes the coefficients to get new wavelet coefficients. The lowpass mixing coefficients for the DWT architecture have spatial size 3×3 and the bandpass coefficients have spatial size 1×1. The DTℂWT architecture takes a single scale DTℂWT and mixes the lowpass and complex bandpass coefficients. Both the lowpass and bandpass coefficients have spatial size 1×1. Numbers are averages over 3 runs.

	CIFAR-10		CIFAR-100		Tiny ImgNet	
	DWT	DTℂWT	DWT	DTℂWT	DWT	DTℂWT
reference	92.6		72.0		59.3	
gainA	93.0	93.0	72.3	72.8	61.3	60.8
gainB	93.0	92.9	72.5	73.4	61.3	61.3
gainC	92.8	93.2	72.1	72.8	60.8	60.7
gainD	92.9	93.3	72.9	73.1	60.3	60.3
gainE	93.3	93.0	72.8	72.7	60.8	60.6
gainF	93.6	93.1	73.6	72.7	61.3	61.3
gainA, gainB	91.9	92.2	70.6	72.3	60.6	60.9
gainB, gainC	92.1	92.6	71.7	73.1	60.3	60.7
gainC, gainD	91.9	92.9	71.0	72.4	60.1	59.9
gainD, gainE	93.1	92.8	72.4	71.9	60.6	60.0
gainA, gainC	92.4	92.8	71.8	73.6	60.7	60.0
gainB, gainD	92.5	92.8	71.7	72.9	60.6	61.2
gainC, gainE	92.4	92.7	71.7	72.2	59.7	60.1
gainA-F						

1.7 Wavelet Based Nonlinearities and Multiple Gain Layers

So far we have only considered doing the mixing operations in the wavelet domain. This is a good starting point, and it is nice to see that we can do apply the gain layer that preserve some of the nice properties of the DTℂWT. Let us call the layer considered so far a **first order gain layer**. Recall this is where a DTℂWT is done, followed by a single linear convolution and then straight away returning to the pixel domain with the inverse DTℂWT. While it is good to see that it is possible to do and even achieves some benefit over a convolutional layer, the proposed layer (B.0.17) can be implemented in the pixel domain as a single convolution.

It would be particularly interesting if we could find a sensible nonlinearity to do in the wavelet domain. This would mean it would be no longer possibile to do the gain layer in the pixel domain. Further, we could then do multiple mixing stages in the wavelet domain before returning to the pixel domain.

But what sensible nonlinearity to use? Two particular options are good initial candidates:

1. The ReLU: this is a mainstay of most modern neural networks and has proved invaluable in the pixel domain. Perhaps its sparsifying properties will work well on wavelet coefficients too.

2. Soft thresholding: a technique commonly applied to wavelet coefficients for denoising and compression. Many proponents of compressed sensing and dictionary learning even like to compare soft thresholding to a two sided ReLU [11], [12].

In this section we will look at each, see if they add to the first order gain layer, and see if they open the possibility of having multiple layers in the wavelet domain.

1.7.1 ReLUs in the Wavelet Domain

A ReLU could be applied to the real lowpass coefficients with ease, but it does not generalize so easily to complex coefficients. One option could be to apply it independently to the real and imaginary coefficients, effectively only selecting one quadrant of the complex plane.

One potential problem with this is that applying a ReLU independently to the real and imaginary components

1.7.2 Non-Linearity

As a first attempt at a non-linearity, we will try a modified L2-norm. In particular, for input w (coming from the convolutional layer), the output y is:

$$y = g(w, b) = \sqrt{\max(0, w_R^2 + w_I^2 - b^2)} \tag{1.7.1}$$

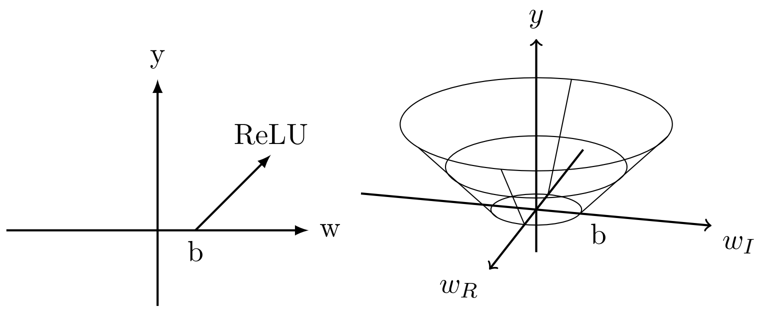

This is an attempt to modify the ReLU nonlinearity by rotating it around the complex plane. Really this is more like the complex generalization of the function $y = \max(0, |x| - b)$, as the ReLU rejects half of the real line, whereas this function only rejects small magnitude values. I justify this like so:

- If a patch of pixels strongly correlates with a filter[2], it will produce a large output.
- A large output will be caught by the ReLU and 'passed' through, with a small subtraction penalty, b.
- If a patch of pixels does not correlate with a filter, it produces a small output, which gets clipped to 0 by the ReLU.
- If a patch of pixels negatively correlates with a filter, say if we multiply a strongly correlated input with -1, then **this should be distinguishable from zero correlation**. A way to do this would be use a soft limiting function ($y = \min(0, x + b) + \max(0, x - b)$), or the rectified version of the soft limiter ($y = \max(0, |x| - b)$.
- The only downside to these non-linearities is that they theoretically 'fire' on much more of the input, which could mean a dramatic change in network behaviour, but really it shouldn't be so drastically different. We can verify this by measuring the probability distribution at the input to non-linearities in a real valued CNN. It is easy to show that they are roughly normally distributed.

1.8 Conclusion and Future Work

In this work we have presented the novel idea of learning filters by taking activations into the wavelet domain, learning mixing coefficients and then returning to the pixel space. This work is done as a preliminary step; we ultimately hope that learning in both the wavelet and pixel space will have many advantages, but as yet it has not been explored. We have

[2]really this should read 'strongly correlates with the mirror image of a filter', but the meaning is the same

considered the possible challenges this proposes and described how a multirate system can learn through backpropagation.

Our experiments so far have been promising. We have shown that our layer can learn in an end-to-end system, achieving very near similar accuracies on CIFAR-10 and CIFAR-100 to the same system with convolutional layers instead. This is a good start and shows the plausibility of such an idea, but we need to search for how to improve these layers if they are to be useful. It will be interesting to see how well we can learn on datasets with larger images - our proposed method naturally learns large kernels, so should scale well with the image size.

In our experiments so far, we only briefly go into the wavelet domain before coming back to the pixel domain to do ReLU nonlinearities, however we plan to explore using nonlinearities in the wavelet domain, such as soft-shrinkage to denoise/sparsify the coefficients [13]. We feel there are strong links between ReLU non-linearities and denoising/sparsity ideas, and that there may well be useful performance gains from mixing real pixel-domain non-linearities with complex wavelet-domain shrinkage functions. Thus we present these ideas here as a starting point for a novel and exciting avenue of deep network research.

References

[1] A. Krizhevsky, I. Sutskever, and G. E. Hinton, “ImageNet Classification with Deep Convolutional Neural Networks”, in *NIPS*, Curran Associates, Inc., 2012, pp. 1097–1105.

[2] S. Marcel and Y. Rodriguez, “Torchvision the Machine-vision Package of Torch”, in *Proceedings of the 18th ACM International Conference on Multimedia*, ser. MM ’10, New York, NY, USA: ACM, 2010, pp. 1485–1488.

[3] S. Fujieda, K. Takayama, and T. Hachisuka, “Wavelet Convolutional Neural Networks for Texture Classification”, *arXiv:1707.07394 [cs]*, Jul. 2017. arXiv: 1707.07394 `[cs]`.

[4] ——, “Wavelet Convolutional Neural Networks”, *arXiv:1805.08620 [cs]*, May 2018. arXiv: 1805.08620 `[cs]`.

[5] T. Guo, H. S. Mousavi, T. H. Vu, and V. Monga, “Deep Wavelet Prediction for Image Super-Resolution”, in *2017 IEEE Conference on Computer Vision and Pattern Recognition Workshops (CVPRW)*, Honolulu, HI, USA: IEEE, Jul. 2017, pp. 1100–1109.

[6] L. Ma, J. Stückler, T. Wu, and D. Cremers, “Detailed Dense Inference with Convolutional Neural Networks via Discrete Wavelet Transform”, *arXiv:1808.01834 [cs]*, Aug. 2018. arXiv: 1808.01834 `[cs]`.

[7] O. Rippel, J. Snoek, and R. P. Adams, “Spectral Representations for Convolutional Neural Networks”, in *Advances in Neural Information Processing Systems 28*, C. Cortes, N. D. Lawrence, D. D. Lee, M. Sugiyama, and R. Garnett, Eds., Curran Associates, Inc., 2015, pp. 2440–2448.

[8] I. W. Selesnick, R. G. Baraniuk, and N. G. Kingsbury, “The dual-tree complex wavelet transform”, *Signal Processing Magazine, IEEE*, vol. 22, no. 6, pp. 123–151, 2005.

[9] N. Kingsbury, “Complex wavelets for shift invariant analysis and filtering of signals”, *Applied and Computational Harmonic Analysis*, vol. 10, no. 3, pp. 234–253, May 2001.

[10] X. Glorot and Y. Bengio, “Understanding the difficulty of training deep feedforward neural networks”, in *In Proceedings of the International Conference on Artificial Intelligence and Statistics (AISTATS’10). Society for Artificial Intelligence and Statistics*, 2010.

[11] V. Papyan, Y. Romano, J. Sulam, and M. Elad, "Theoretical Foundations of Deep Learning via Sparse Representations: A Multilayer Sparse Model and Its Connection to Convolutional Neural Networks", *IEEE Signal Processing Magazine*, vol. 35, no. 4, pp. 72–89, Jul. 2018.

[12] V. Papyan, Y. Romano, and M. Elad, "Convolutional Neural Networks Analyzed via Convolutional Sparse Coding", *arXiv:1607.08194 [cs, stat]*, Jul. 2016. arXiv: 1607.08194 `[cs, stat]`.

[13] D. L. Donoho and J. M. Johnstone, "Ideal spatial adaptation by wavelet shrinkage", en, *Biometrika*, vol. 81, no. 3, pp. 425–455, Sep. 1994.

[14] D. Kingma and J. Ba, "Adam: A Method for Stochastic Optimization", *arXiv:1412.6980 [cs]*, Dec. 2014. arXiv: 1412.6980 `[cs]`.

Appendix A

Invertible Transforms and Optimization

To see this, let us consider the work from [7] where filters are parameterized in the Fourier domain.

If we define the DFT as the orthonormal version, i.e. let:

$$U_{ab} = \frac{1}{\sqrt{N}} \exp\{\frac{-2j\pi ab}{N}\}$$

then call $X = \mathrm{DFT}\{x\}$. In matrix form the 2-D DFT is then:

$$\begin{aligned} X &= \mathrm{DFT}\{x\} = UxU && \text{(A.0.1)} \\ x &= \mathrm{DFT}^{-1}\{X\} = U^*YU^* && \text{(A.0.2)} \end{aligned}$$

When it comes to gradients, these become:

$$\begin{aligned} \frac{\partial L}{\partial X} &= U\frac{\partial L}{\partial x}U = \mathrm{DFT}\left\{\frac{\partial L}{\partial x}\right\} && \text{(A.0.3)} \\ \frac{\partial L}{\partial x} &= U^*\frac{\partial L}{\partial X}U^* = \mathrm{DFT}^{-1}\left\{\frac{\partial L}{\partial X}\right\} && \text{(A.0.4)} \end{aligned}$$

Now consider a single filter parameterized in the DFT and spatial domains presented with the exact same data and with the same ℓ_2 regularization ϵ and learning rate η. Let the spatial filter at time t be $\mathbf{w}_t$, the Fourier-parameterized filter be $\hat{\mathbf{w}}_t$, and let

$$\hat{\mathbf{w}}_1 = \mathrm{DFT}\{\mathbf{w}_1\} \tag{A.0.5}$$

After presenting both systems with the same minibatch of samples $\mathcal{D}$ and calculating the gradient $\frac{\partial L}{\partial \mathbf{w}}$ we update both parameters:

$$\begin{aligned}
\mathbf{w}_2 &= \mathbf{w}_1 - \eta\left(\frac{\partial L}{\partial \mathbf{w}} + \epsilon \mathbf{w}_1\right) && \text{(A.0.6)}\\
&= (1-\eta\epsilon)\mathbf{w}_1 - \eta\frac{\partial L}{\partial \mathbf{w}} && \text{(A.0.7)}\\
\hat{\mathbf{w}}_2 &= \hat{\mathbf{w}}_1 - \eta\left(\frac{\partial L}{\partial \hat{\mathbf{w}}} + \epsilon \hat{\mathbf{w}}_1\right) && \text{(A.0.8)}\\
&= (1-\eta\epsilon)\hat{\mathbf{w}}_1 - \eta\frac{\partial L}{\partial \hat{\mathbf{w}}} && \text{(A.0.9)}\\
& && \text{(A.0.10)}
\end{aligned}$$

Where we have shortened the gradient of the loss evaluated at the current parameter values to $\delta_{\mathbf{w}}$ and $\delta_{\hat{\mathbf{w}}}$. We can then compare the effect the new parameters would have on the next minibatch by calculating $\text{DFT}^{-1}\{\hat{\mathbf{w}}_2\}$. Using equations A.0.3 and A.0.5 we then get:

$$\begin{aligned}
\text{DFT}^{-1}\{\hat{\mathbf{w}}_2\} &= \text{DFT}^{-1}\left\{(1-\eta\epsilon)\hat{\mathbf{w}}_1 - \eta\,\frac{\partial L}{\partial \hat{\mathbf{w}}}\right\} && \text{(A.0.11)}\\
&= (1-\eta\epsilon)\mathbf{w}_1 - \eta\ \text{DFT}^{-1}\left\{\frac{\partial L}{\partial \hat{\mathbf{w}}}\right\} && \text{(A.0.12)}\\
&= (1-\eta\epsilon)\mathbf{w}_1 - \eta\frac{\partial L}{\partial \mathbf{w}} && \text{(A.0.13)}\\
&= \mathbf{w}_2 && \text{(A.0.14)}
\end{aligned}$$

A.0.1 Regularization

If we use ℓ_1 then the above doesn't hold.

A.0.2 Optimization

If we us adam things r different.

This does not hold for the Adam [14] or Adagrad optimizers, which automatically rescale the learning rates for each parameter based on estimates of the parameter's variance. Rippel et. al. use this fact in their paper [7].

Appendix B

DTℂWT **Single Subband Gains**

Let us consider one subband of the DTℂWT. This includes the coefficients from both tree A and tree B. For simplicity in this analysis we will consider the 1-D DTℂWT without the channel parameter c. If we only keep coefficients from a given subband and set all the others to zero, then we have a reduced tree as shown in Figure B.1. The end to end transfer function is:

$$\frac{Y(z)}{X(z)} = \frac{1}{M} \sum_{k=0}^{M-1} \left[A(W^k z) C(z) + B(W^k z) D(z) \right] \tag{B.0.1}$$

where the aliasing terms are formed from the addition of the rotated z transforms, i.e. when $k \neq 0$.

Theorem B.1. *Suppose we have complex filters $P(z)$ and $Q(z)$ with support only in the positive half of the frequency space. If $A(z) = 2\mathrm{Re}\,(P(z))$, $B(z) = 2\mathrm{Im}\,(P(z))$, $C(z) = 2\mathrm{Re}\,(Q(z))$ and $D(z) = -2\mathrm{Im}\,(Q(z))$, then the aliasing terms in* (B.0.1) *are nearly zero and the system is nearly shift invariant.*

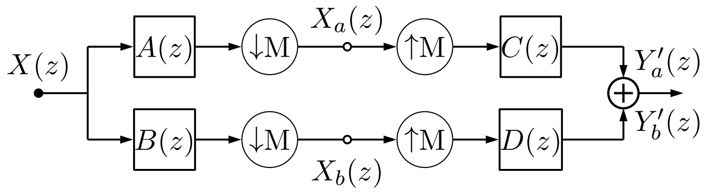

Figure B.1: **Block Diagram of 1-D** DTℂWT**.** Note the top and bottom paths are through the wavelet or scaling functions from just level m ($M = 2^m$). Figure based on Figure 4 in [9].

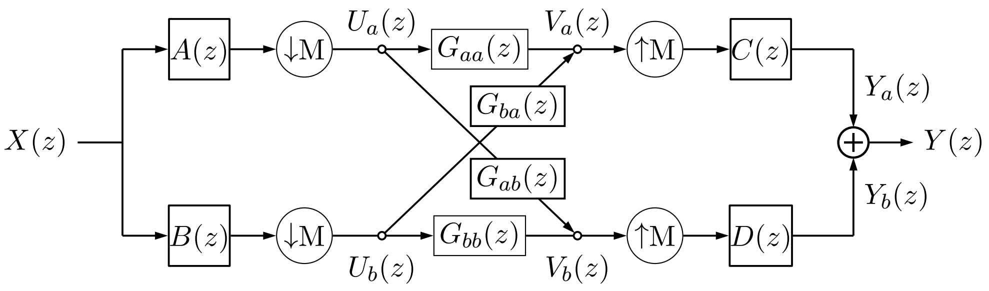

Figure B.2: **Block Diagram of 1-D** DTℂWT**.** Note the top and bottom paths are through the wavelet or scaling functions from just level m ($M = 2^m$). Figure based on Figure 4 in [9].

Proof. See section 4 of [9] for the full proof of this, and section 7 for the bounds on what 'nearly' shift invariant means. In short, from the definition of A, B, C and D it follows that:

$$\begin{aligned} A(z) &= P(z) + P^*(z) \\ B(z) &= -j(P(z) - P^*(z)) \\ C(z) &= Q(z) + Q^*(z) \\ D(z) &= j(Q(z) - Q^*(z)) \end{aligned}$$

where $H^*(z) = \sum_n h^*[n]z^{-n}$ is the Z-transform of the complex conjugate of the complex filter h. This reflects the purely positive frequency support of $P(z)$ to a purely negative one. Substituting these into (B.0.1) gives:

$$A(W^k z)C(z) + B(W^k z)D(z) = 2P(W^k z)Q(z) + 2P^*(W^k z)Q^*(z) \tag{B.0.2}$$

Using (B.0.2), Kingsbury shows that it is easier to design single side band filters so $P(W^k z)$ does not overlap with $Q(z)$ and $P^*(W^k z)$ does not overlap with $Q^*(z)$ for $k \neq 0$. □

Using Theorem B.1 (B.0.1) reduces to:

$$\begin{aligned} \frac{Y(z)}{X(z)} &= \frac{1}{M}\left[P(z)Q(z) + P^*(z)Q^*(z)\right] && \text{(B.0.3)} \\ &= \frac{1}{M}\left[A(z)C(z) + B(z)D(z)\right] && \text{(B.0.4)} \end{aligned}$$

Let us extend this idea to allow for any linear gain applied to the passbands (not just zeros and ones). Ultimately, we may want to allow for nonlinear operations applied to the wavelet coefficients, but we initially restrict ourselves to linear gains so that we can build from a sensible base. In particular, if we want to have gains applied to the wavelet coefficients, it would be nice to maintain the shift invariant properties of the DTℂWT.

Figure B.2 shows a block diagram of the extension of the above to general gains. This is a two port network with four individual transfer functions. Let the transfer fucntion from U_i

to V_j be G_{ij} for $i, j \in \{a, b\}$. Then V_a and V_b are:

$$\begin{aligned} V_a(z) &= U_a(z)G_{aa}(z) + U_b(z)G_{ba}(z) && \text{(B.0.5)} \\ &= \frac{1}{M}\sum_k X(W^k z^{1/k})\left[A(W^k z^{1/k})G_{aa}(z) + B(W^k z^{1/k})G_{ba}(z)\right] && \text{(B.0.6)} \\ V_b(z) &= U_a(z)G_{ab}(z) + U_b(z)G_{bb}(z) && \text{(B.0.7)} \\ &= \frac{1}{M}\sum_k X(W^k z^{1/k})\left[A(W^k z^{1/k})G_{ab}(z) + B(W^k z^{1/k})G_{bb}(z)\right] && \text{(B.0.8)} \end{aligned}$$

Further, Y_a and Y_b are:

$$\begin{aligned} Y_a(z) &= C(z)V_a(z^M) && \text{(B.0.9)} \\ Y_b(z) &= D(z)V_b(z^M) && \text{(B.0.10)} \end{aligned}$$

Then the end to end transfer function is:

$$\begin{aligned} Y(z) = Y_a(z) + Y_b(z) = \frac{1}{M}\sum_{k=0}^{M-1} X(W^k z)\Big[&A(W^k z)C(z)G_{aa}(z^k) + B(W^k z)D(z)G_{bb}(z) + \\ &B(W^k z)C(z)G_{ba}(z^k) + A(W^k z)D(z)G_{ba}(z)\Big] \end{aligned} \tag{B.0.11}$$

Theorem B.2. *If we let $G_{aa}(z^k) = G_{bb}(z^k) = G_r(z^k)$ and $G_{ab}(z^k) = -G_{ba}(z^k) = G_i(z^k)$ then the end to end transfer function is shift invariant.*

Proof. Using the above substitutions, the terms in the square brackets of (B.0.11) become:

$$G_r(z^k)\left[A(W^k z)C(z) + B(W^k z)D(z)\right] + G_i(z^k)\left[A(W^k z)D(z) - B(W^k z)C(z)\right] \tag{B.0.12}$$

Theorem B.1 already showed that the G_r terms are shift invariant and reduce to $A(z)C(z) + B(z)D(z)$. To prove the same for the G_i terms, we follow the same procedure. Using our definitions of A, B, C, D from Theorem B.1 we note that:

$$\begin{aligned} A(W^k z)D(z) - B(W^k z)C(z) &= j\left[P(W^k z) + P^*(W^k z)\right][Q(z) - Q^*(z)] + && \text{(B.0.13)} \\ &\quad j\left[P(W^k z) - P^*(W^k z)\right][Q(z) + Q^*(z)] && \text{(B.0.14)} \\ &= 2j\left[P(W^k z)Q(z) - P^*(W^k z)Q^*(z)\right] && \text{(B.0.15)} \end{aligned}$$

We note that the difference between the G_r and G_i terms is just in the sign of the negative frequency parts, $AD - BC$ is the Hilbert pair of $AC + BD$. To prove shift invariance for the G_r terms in Theorem B.1, we ensured that $P(W^k z)Q(z) \approx 0$ and $P^*(W^k z)Q^*(z) \approx 0$ for $k \neq 0$. We can use this again here to prove the shift invariance of the G_i terms in (B.0.12). This completes our proof. □

Using Theorem B.2, the end to end transfer function with the gains is now

$$\frac{Y(z)}{X(z)} = \frac{2}{M}\Big[G_r(z^M)\,(A(z)C(z)+B(z)D(z))+G_i(z^M)\,(A(z)D(z)-B(z)C(z))\Big] \tag{B.0.16}$$

$$= \frac{2}{M}\Big[G_r(z^M)\,(PQ+P^*Q^*)+jG_i(z^M)\,(PQ-P^*Q^*)\Big] \tag{B.0.17}$$

Now we know can assume that our DTℂWT is well designed and extracts frequency bands at local areas, then our complex filter $G(z)=G_r(z)+jG_i(z)$ allows us to modify these passbands (e.g. by simply scaling if $G(z)=C$, or by more complex functions.

Appendix C

Complex Convolution and Gradients

Consider a complex number $z = x + iy$, and the complex mapping

$$w = f(z) = u(x,y) + iv(x,y)$$

where u and v are called 'conjugate functions'. Let us examine the properties of $f(z)$ and its gradient.

The definition of gradient for complex numbers is:

$$\lim_{\Delta z \to 0} \frac{f(z+\Delta z) - f(z)}{\Delta z}$$

A necessary condition for $f(z,\bar{z})$ to be an analytic function is $\frac{\partial f}{\partial \bar{z}} = 0$. I.e. f must be purely a function of z, and not $\bar{z}$.

A geometric interpretation of complex gradient is shown in Figure C.1. As Δz shrinks to 0, what does Δw converge to? E.g. consider the gradient of approach $m = \frac{dy}{dx} = \tan\theta$, then the derivative is

$$\gamma = \alpha + i\beta = D(x,y) + P(x,y)e^{-2i\theta}$$

where

$$\begin{aligned} D(x,y) &= \frac{1}{2}(u_x + v_y + i(v_x - u_y)) \qquad \text{(C.0.1)} \\ P(x,y) &= \frac{1}{2}(u_x - v_y + i(v_x + u_y)) \qquad \text{(C.0.2)} \end{aligned}$$

$P(x,y) = \frac{dw}{d\bar{z}}$ needs to be 0 for the function to be analytic. This is where we get the Cauchy-Riemann equations:

$$\frac{\partial u}{\partial x} = \frac{\partial v}{\partial y}\frac{\partial u}{\partial y} = -\frac{\partial v}{\partial x} \quad \text{(C.0.3)}$$

The function $f(z)$ is analytic (or regular or holomorphic) if the derivative $f'(z)$ exists at all points z in a region R. If R is the entire z-plane, then f is entire.

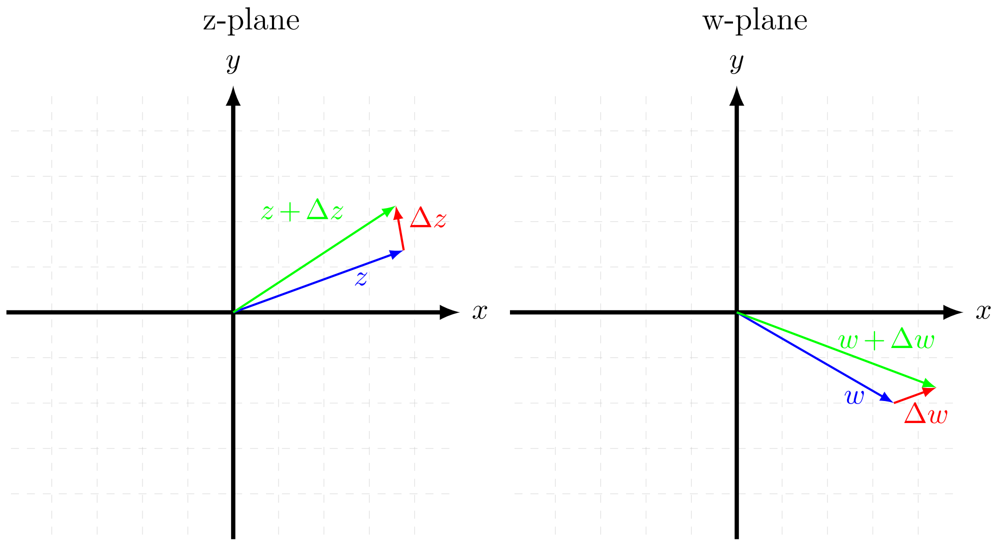

Figure C.1: **Geometric interpretation of complex gradient.** The gradient is defined as $f'(z) = \lim_{\Delta z \to 0} \frac{\Delta w}{\Delta z}$. It must approach the same value independent of the direction Δz approaches zero. This turns out to be a very strong and somewhat restrictive property.

C.1 Grad Operator

Recall, the gradient is a multi-variable generalization of the derivative. The gradient is a vector valued function. In the case of complex numbers, it can be represented as a complex number too. E.g. consider $W(z) = F(x,y)$ (note that in general it may be simple to find F given G, but they are different functions).

I.e.

$$\nabla F = \frac{\partial F}{\partial x} + i\frac{\partial F}{\partial y}$$

Consider the case when F is purely real, then $F(x,y) = F(\frac{z+\bar{z}}{2}, \frac{z-\bar{z}}{2i}) = G(z,\bar{z})$ Then

$$\nabla F = \frac{\partial F}{\partial x} + i\frac{\partial F}{\partial y} = 2\frac{\partial G}{\partial \bar{z}}$$

If F is complex, let $F(x,y) = P(x,y) + iQ(x,y) = G(z,\bar{z})$, then

$$\nabla F = \left(\frac{\partial}{\partial x} + i\frac{\partial}{\partial y}\right)(P+iQ) = \left(\frac{\partial P}{\partial x} - \frac{\partial Q}{\partial x}\right) + i\left(\frac{\partial P}{\partial y} + \frac{\partial Q}{\partial x}\right) = 2\frac{\partial G}{\partial \bar{z}}$$

It is clear to see how the purely real case is a subset of this (set Q=0 and all its partials will be 0 too).

If G is an analytic function, then $\frac{\partial G}{\partial \bar{z}} = 0$ and so the gradient is 0, and the Cauchy-Riemann equations hold $\frac{\partial P}{\partial x} = \frac{\partial Q}{\partial y}$ and $\frac{\partial P}{\partial y} = -\frac{\partial Q}{\partial x}$

C.2 Hilbert Pairs of General Functions

How does this affect me? I don't think I'll be able to use analytic non-linearities, however I may be able to have analytic filters, like those of the DTℂWT.

The Hilbert pair of the cosine is the sine function, but what about in general? If $x = \delta(t)$, its Hilbert pair $jy = \frac{-j}{\pi t}$. Like the dirac delta function, this also has a flat spectrum, and the figure for it is shown below.

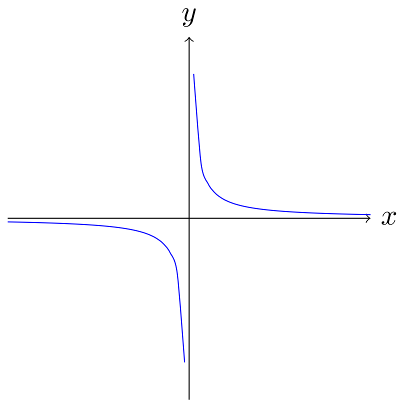

That means if we wanted to get the Hilbert pair of a sampled signal, then we would have to add shifts and scales of y, which unfortunately has infinite support. We would also have to lowpass it, as we do for the sampled version (so their frequency spectrums are the same).

C.3 Usefulness of Complex Numbers

Nick made a good point in our recent meeting that when trying to use the complex plane, we must know/understand what it is we want to gain from the added representation. For the case of the DTCWT, he converted the non-analytic sinusoids of the wavelet transform into an analytic signal.

I.e. let us ignore the previous notation of $x = \mathrm{Re}(z), y = \mathrm{Im}(z)$ and redefine them to indicate the horizontal and vertical directions in an image.

For a real wavelet transform, all of the cosine terms are:

$$\cos\omega_1 x = \frac{1}{2}\left(e^{j\omega_1 x} + e^{-j\omega_1 x}\right) \tag{C.3.1}$$

If we consider $z_x = e^{j\omega_1 x}$, then this is clearly a function of both z_x and its conjugate (as are all real valued functions). I.e. $\cos\omega_1 x = F(z_x, \bar{z_x})$. Nick replaced this with the analytic equivalent of this function by adding in the Hilbert pair term.

$$\cos\omega_1 x + j\sin\omega_1 x = e^{j\omega_1 x} = F(z_x) \tag{C.3.2}$$

From our above definitions of analytic functions, it is clear to see that this is now no longer a function of the conjugate term $\bar{z_x}$, so it is analytic. The benefit for Nick was that now he could separably multiply the x and the y sinusoids to get:

$$e^{j\omega_1 x} \times e^{j\omega_2 y} = F(z_x)F(z_y) = e^{j(\omega_1 x + \omega_2 y)} = F(z_x + z_y) \tag{C.3.3}$$

Also, I must be careful with regularizing complex weights. We want to set some of the weights to 0, and let the remaining ones evolve to whatever phase they please. To do this, either use the L-2 norm on the real and imaginary parts independently, or be careful about using the L-1 norm. This is because we really want to be penalising the magnitude of the complex weights, r and:

$$\|r\|_2^2 = \left\|\sqrt{x^2+y^2}\right\|_2^2 = \sum x^2 + y^2 = \sum x^2 + \sum y^2 = \|x\|_2^2 + \|y\|_2^2 \tag{C.3.4}$$

But this wouldn't necessarily be the case for the L-1 norm case.

C.4 Working with Complex weights in CNNs

As a first pass, I think I shouldn't concern myself too much with analytic functions and having the Cauchy-Riemann equations met. Instead, I will focus on implementing the CNN with a real and imaginary component to the filters, and have these stored as independent variables.

Unfortunately, most current neural network tools only work with real numbers, so we must write out the equations for the forward and backwards passes, and ensure ourselves that we can achieve the equivalent of a complex valued filter.

C.5 Forward pass

C.5.1 Convolution

In the above example **f** has a spatial support of only 1×1. We still were able to get a somewhat complex shape by shifting the relative phases of the complex coefficients, but we are inherently limited (as we can only rotate the coefficient by at most 2π). So in general, we want to be able to consider the family of filters $\mathbf{f} \in \mathbb{C}^{m_1 \times m_2 \times C}$. For ease, let us consider only square filters of spatial support m, so $\mathbf{f} \in \mathbb{C}^{m \times m \times C}$. Note that we have restricted the third dimension of our filter to be $C = 12$ in this case. This means that convolution is only in the spatial domain, rather than across channels. Ultimately we would like to be able to handle the more general case of allowing the filter to rotate through channels, but we will tackle the simpler problem first[1]

Let us represent the complex input with z, which is of shape $\mathbb{C}^{n_1 \times n_2 \times C}$. We call w the result we get from convolving **z** with **f**, so $\mathbf{w} \in \mathbb{C}^{n_1+m-1, n_2+m-1, 1}$. With appropriate zero or symmetric padding, we can make w have the same spatial shape as **z**. Now, consider the full complex convolution to get w:

$$w[l_1, l_2] = \sum_{c=0}^{C-1} \sum_{k_1,k_2} f[k_1, k_2, c] z[l_1 - k_1, l_2 - k_2, c] \tag{C.5.1}$$

Let us define

$$z = z_R + j z_I \tag{C.5.2}$$
$$w = w_R + j w_I \tag{C.5.3}$$
$$f = f_R + j f_I \tag{C.5.4}$$

[1]Recall from **??**, the benefit of allowing a filter to rotate through the channel dimension was we could easily obtain 30° shifts of the sensitive shape.

where all of these belong to the real space of the same dimension as their parent. Then

$$\begin{aligned}
w[l_1,l_2] &= w_R + jw_I && \text{(C.5.5)}\\
&= \sum_{c=0}^{C-1}\sum_{k_1,k_2} f[k_1,k_2,c]z[l_1-k_1,l_2-k_2,c] && \text{(C.5.6)}\\
&= \sum_{c=0}^{C-1}\sum_{k_1,k_2} (f_R[k_1,k_2,c]+jf_I[k_1,k_2,c])(z_R[l_1-k_1,l_2-k_2,c]+jz_I[l_1-k_1,l_2-k_2,c]) && \text{(C.5.7)}\\
&= \sum_{c=0}^{C-1}\sum_{k_1,k_2} (z_R[l_1-k_1,l_2-k_2,c]f_R[k_1,k_2,c]-z_I[l_1-k_1,l_2-k_2,c]f_I[k_1,k_2,c]) && \text{(C.5.8)}\\
&+ j\sum_{c=0}^{C-1}\sum_{k_1,k_2} (z_R[l_1-k_1,l_2-k_2,c]f_I[k_1,k_2,c]+z_I[l_1-k_1,l_2-k_2,c]f_R[k_1,k_2,c]) && \text{(C.5.9)}\\
&= ((z_R * f_R)-(z_I * f_I))[l_1,l_2]+((z_R * f_I)+(z_I * f_R))[l_1,l_2] && \text{(C.5.10)}
\end{aligned}$$

Unsurprisingly, complex convolution is then the sum and difference of 4 real convolutions.

C.6 Backwards Pass

Now we need to calculate what the complex gradients will be, and importantly, how to implement them using only real representations.

A typical loss function is:

$$\begin{aligned}
\mathcal{L} &= \mathcal{L}_{\text{data}} + \mathcal{L}_{\text{reg.}} && \text{(C.6.1)}\\
&= \frac{1}{N}\sum_{n=0}^{N-1}\sum_{k} y_{nk}\log\pi_{nk} + \lambda\sum_{l}\theta_l^2 && \text{(C.6.2)}
\end{aligned}$$

The derivative of the regularizer loss w.r.t. the parameters is trivial to find, so let us only focus on the data loss for now.